The Wave Digital Tonehole Model

Maarten van Walstijn

Faculty of Music, University of Edinburgh
12 Nicholson Square, Edinburgh EH8 9DF

Gary Scavone

CCRMA, Music Dept., Stanford University,
Stanford, CA 94305 USA

Abstract—This paper presents a discrete-time model for simulation of woodwind toneholes in a musical sound synthesis context. Starting from a lumped element approximation of the partially open tonehole, we develop an efficient digital tonehole model with dynamically adjustable tonehole state. The model, that covers a wider range of woodwind toneholes than those previously reported, is discretised with the use of wave digital filter techniques.

INTRODUCTION

Physical modelling of woodwind instruments with application to musical sound synthesis requires a digital tonehole model that 1) can represent toneholes of any physically and musically feasible dimensions, 2) can be applied in the efficient travelling-wave formulation (such as a digital waveguide model), 3) closely approximates acoustical tonehole theories in the low-frequency-limit, 4) characterises all tonehole states from open to closed, and 5) is computationally efficient. Tonehole models that were previously developed in this context [5, 7, 8, 9, 10] do not meet all of these requirements. The three-port tonehole model described in [9], in which wave propagation in the tonehole is modelled using a short delay-line, meets all criteria except the first. This is because the model is only computable for tonehole lengths that correspond to a round-trip time of at least one delay. For an audio sampling frequency $f_s = 44.1$kHz and a wave velocity $c = 342$m/s, the tonehole length is restricted to a minimum of $t = c/(2f_s) \approx 3.8$mm. Since increasing the sample rate is undesirable for a variety of reasons, simulation of woodwind instruments that contain holes of shorter length (such as the saxophone) requires an alternative modelling approach.

WAVE DIGITAL MODELLING

Wave digital filter (WDF) techniques are used for digital simulation of analog networks [1, 2]. The resulting digital networks are called *wave digital filters*. The classical analogy between electric and acoustic systems allows application of similar techniques for the discretisation of lumped elements in an acoustic model. WDF techniques are similar to digital waveguide modelling (DWM) techniques in the sense that they both digitise continuous-time models using *wave variables*. A combined approach ("wave digital modelling") is possible in which *lumped* elements are modelled using WDF techniques and *distributed* elements are modelled using DWM techniques. For example, in [6], such an approach has been taken for digital simulation of force interaction between hammer and string in a piano. In the current context of modelling acoustic wind instruments, the instantaneous acoustic variables are pressure (P) and volume flow (U). We define the decompostion of these into wave variables as:

$$P^+ = \frac{P + RU}{2}$$

$$P^- = \frac{P - RU}{2},$$

$$(1)$$

where R is the *port-resistance*. In the case of a distributed acoustic element, the wave variables correspond to pressure-waves travelling through a certain medium. The port-resistance then equals the reference impedance that characterises the medium (as in DWM). In the lumped case, the waves may only be understood to be travelling instantaneously [6]. From an acoustical point of view, the port-resistance may then be considered arbitrary. Similar to the derivation of WDFs (as described in [1, 2]), this freedom of choice can be used to avoid delay-free loops in the final discrete-time modelling structure.

1

THE HALF-HOLE MODEL

Figure 1 shows a cross-sectional view of a woodwind tonehole. In the low-frequency limit, the hole dimensions are usually small in comparison with the acoustic wavelength, thus the acoustic behaviour may be characterised by a lumped acoustic element. For an open hole, the behaviour is approximately that of a pure inertance, while for a closed one it approximately corresponds to a pure compliance [10]. For intermediate
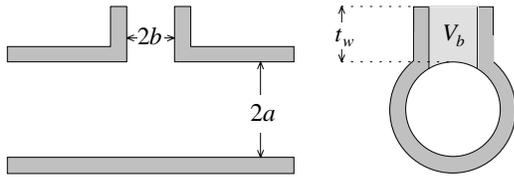

Figure 1: Cross-sections of a woodwind tonehole.

tonehole states (partially open holes or "half-holes"), the tonehole volume V_b can be divided into an "open part" that behaves as an inertance, and a "closed part" that behaves as a compliance. These volumes operate in parallel, thus the half-hole load impedance is:

$$Z_s(\omega) = \frac{j\omega L}{1 - \omega^2 LC}, \qquad (2)$$

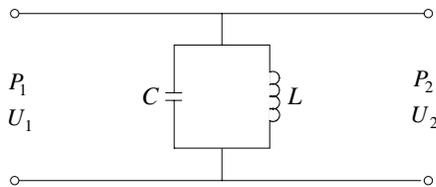Figure 2 shows the network equivalent of this model. The half-hole compliance (C) and inertance (L) are

Figure 2: Electrical network representation of the half-hole model.

given by:

$$C = (1 - g) \cdot \frac{S_b t}{\rho c^2} \quad , \quad L = \frac{\rho t_e}{g S_b}, \qquad (3)$$

where the parameter g expresses the tonehole state, defined as the ratio between *open* and *total* tonehole volume. The tonehole height t is defined such that its product with the tonehole surface S_b equals the geometric volume V_b [3]:

$$t = t_w + 0.125b(b/a)\left(1 + 0.172(b/a)^2\right), \qquad (4)$$

The tonehole effective length t_e is similar to t, though it includes inner and outer length-correction terms.

The value for t_e given in [3] is frequency-dependent, though at low frequencies the following approximation is sufficiently accurate:

$$t_e = t + b\left(1.4 - 0.58(b/a)^2\right) \qquad (5)$$

An additional effect of inserting a hole in a woodwind bore is that the effective acoustic length of the bore is slightly reduced on both sides of the hole [3, 10]. This length-correction depends on the tonehole *series equivalent length*, for which we found a simplified expression that applies to both open and closed tonehole state:

$$t_a = \frac{0.47b(b/a)^4}{1 + 0.62(b/a)^2 + 0.64(b/a)} \qquad (6)$$

The total main bore negative length correction for a tonehole with series equivalent length t_a is $l_a = -(a/b)^2 t_a$ [3]. Thus if the lengths of the main bore sections on each side of the tonehole are l_1 and l_2, they should be corrected to $l_1 + l_a/2$ and $l_2 + l_a/2$, respectively. Because the length-correction is very small, this formulation differs only slightly from the series impedance formulation in [3].

DISCRETISATION

In order to represent a half-hole model in a wave digital modelling context, a decomposition of the instantaneous variables (P and U) into wave variables is required. Taking a three-port modelling approach (as described in [5, 7, 9]), and applying eqs. (1) to the network in figure 2, the modelling structure depicted in figure 3 results. Because the main bore is modelled as a digital waveguide, both R_1 and R_2 must equal the main bore characteristic impedance Z_0. The scattering equations of the three-port junction that models the wave interaction at the intersection between the main bore and the tonehole are:

$$
\begin{aligned}
P_1^- &= P_2^- + W \\
P_2^+ &= P_1^+ + W \\
P_3^+ &= P_1^+ + P_2^- - P_3^- + W,
\end{aligned}
\qquad (7)
$$

with

$$W = \left(\frac{-Z_0}{2R_3 + Z_0}\right)\left[P_1^+ + P_2^- - 2P_3^-\right], \qquad (8)$$

where the lumped element port-resistance R_3 has to be chosen such that the structure is computable. The continuous-time tonehole "reflectance" $R_s(\omega)$ is:

$$R_s(\omega) = \frac{Z_s(\omega) - R_3}{Z_s(\omega) + R_3} \qquad (9)$$

Note that $R_s(\omega)$ does not correspond to the actual physical tonehole reflectance as seen from the main
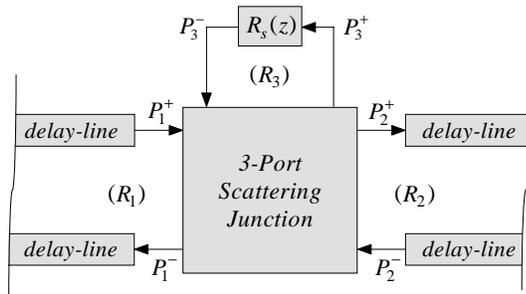
Figure 3: Structure for discrete-time modelling of the half-hole model. The delay-lines model wave propagation in the main bore.

bore. Substitution of eq. (2) and applying the bilinear transform gives the wave digital reflectance, which has the form of an all-pass filter:

$$R_s(z) = -\frac{\alpha_1 + \alpha_2 z^{-1} + z^{-2}}{1 + \alpha_2 z^{-1} + \alpha_1 z^{-2}}, \qquad (10)$$

with

$$\alpha_1 = \frac{R_3\left(1 + \beta^2 LC\right) - \beta L}{R_3\left(1 + \beta^2 LC\right) + \beta L}$$

$$\alpha_2 = \frac{2R_3\left(1 - \beta^2 LC\right)}{R_3\left(1 + \beta^2 C\right) + \beta L}, \qquad (11)$$

where $\beta = 2f_s$ is the bilinear operator. In order to avoid a delay-free loop, R_3 must be chosen such that the wave P_3^+ entering $R_s(z)$ is not immediately reflected back towards the three-port scattering junction via P_3^-. This requires setting the filter coefficient $\alpha_1 = 0$, which means that we must choose $R_3 = \beta/(L^{-1} + \beta^2 C)$. The resulting digital reflectance is:

$$R_s(z) = -z^{-1}\left(\frac{\alpha_2 + z^{-1}}{1 + \alpha_2 z^{-1}}\right), \qquad (12)$$

with

$$\alpha_2 = \frac{L^{-1} - \beta^2 C}{L^{-1} + \beta^2 C}. \qquad (13)$$

Both R_3 and α_2 are computed using the term L^{-1}, so that we can let $L \to \infty$ (which corresponds to fully closing the tonehole). In order to investigate the effect of the discretisation, the half-hole *two-port reflectance* (i.e., the reflectance P_1^-/P_1^+) of the half-hole was computed for a range of tonehole states. Figure 4 compares the continuous-time half-hole model with its digital version, the "wave digital tonehole model", in terms of magnitude response. As can be expected, the discrete-time model closely approximates the continuous-time model at the lower frequencies. However, the deviation is rather large at the higher frequencies. Fortunately, this discrepancy is relatively insignificant in a full instrument implementation, because the air column reflection function is strongly low-pass due to viscothermal and radiation losses.
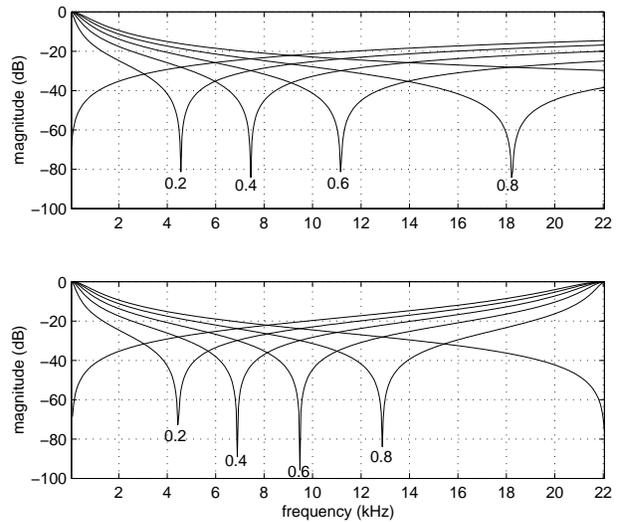

Figure 4: Two-port reflectance of the continuous-time (top) and the discrete-time (bottom) half-hole model, for a range of tonehole states ($g = 0.0, 0.2, 0.4, 0.6, 0.8, 1.0$).

APPLICATION TO A SIX-HOLE FLUTE

The wave digital (WD) tonehole model closely approximates the tonehole transmission-line model described in [3]. This was verified by comparing the reflection function of a six-hole flute, as computed in [3], with the reflection function of a WD model of the flute. Figure 5 displays this comparison for a fingering that corresponds to the note G. A 5kHz low-pass filter was applied to both reflection functions in order to facilitate a visual comparison. In the WD model, fractional delay-lengths were modelled using third-order Lagrange interpolation filters [5], which have a negligible error in a bandwidth of 5kHz. In order to further ensure that the comparison is focussed on the tonehole part of the model, viscothermal losses were neglected in both computations. Note that the fit is so close that
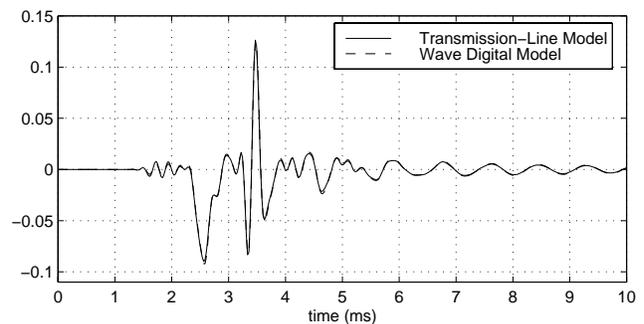

Figure 5: Six-hole flute reflection function for the note G (the first three holes closed).

the difference between the curves is barely visible.

SOUND RADIATION

Sound is radiated from a fully or partially open tonehole because the air just outside the tonehole is disturbed by the vibrational motion of the "open" part of the tonehole volume. Hence the flow U_e exiting the hole equals the flow through the inertance:

$$U_e = \frac{P_3}{j\omega L} \qquad (14)$$

A woodwind tonehole may be considered as an isotropic source [4]. Given a source-strength U_e, the radiation pressure at a distance r from such a source is:

$$P_{rad}(r) = \left(\frac{j\omega\rho}{4\pi r}\right) U_e\, e^{-jkr}, \qquad (15)$$

where $k = \omega/c$ is the free space wave velocity. By combining (14) and (15), we can compute the pressure radiated from a woodwind tonehole as:

$$P_{rad}(r) = \left(\frac{\rho}{4\pi r L}\right) P_3\, e^{-jkr} \qquad (16)$$

Note that the frequency term $j\omega$ has disappeared in the final result. The term e^{-jkr} represents a pure time-delay (i.e., the time it takes for a radiated pressure wave to reach the "listening point"). Thus, the radiated pressure at any distance from the tonehole can be computed by simply *scaling* and *delaying* the bore pressure P_3 just underneath the tonehole. We can incorporate this into the wave digital tonehole model by formulating the digital domain version of (16) as:

$$P_{rad}(r) = \left(\frac{g}{r}\right) \xi\, P_3\, z^{-N}, \qquad (17)$$

where z^{-N} represents a delay-line of fractional length $N = r/(cT)$, and where $\xi = S_b/(4\pi t_e)$ is a constant. It must be noted that eq. (17) gives a good approximation at lower frequencies, but the accuracy decreases for higher frequencies. This is mainly because the WD tonehole model is based on a low-frequency approximation of the real acoustical behaviour of the tonehole. Moreover, we have assumed that the radiation is isotropic (i.e., the flow spreads out evenly in all directions). This assumption is valid for low frequencies, but for higher frequencies the effects of directivity need to be taken into account (such as described in [11]). Since the higher frequencies are relevant from a perceptual point of view, an extra filter (that compensates for the deviations described above) can be applied to the pressure calculated with eq. (17) in order to obtain a better aural result. In general, such a filter has a rather "smooth" high-pass amplitude response, and can be approximated with a lower-order digital filter.

CONCLUSIONS

The WD tonehole model uses only two multiplications per sample (one for the three-port scattering and one for the reflectance filter). Similar to the three-port tonehole model presented in [9], the model allows dynamic control of the tonehole state and closely approximates the established theories on tonehole acoustics. The advantages of the WD model are that 1) there is no minimum tonehole length, which allows simulation of toneholes of particular small dimensions and 2) no fractional delay filters are required for implementation of fractional delay tonehole lengths.

REFERENCES

[1] Fettweis, A. 1986. *Wave Digital Filters. Proc. of the IEEE*, Vol. 74 (2), pp. 270–327.

[2] Lawson, S., and Mirzai, A. 1990. *Wave Digital Filters.* Ellis Horwood, New York.

[3] Keefe, D.H. 1990. Woodwind air column models. *JASA* 88(1), pp. 35–51.

[4] Fletcher N.H., and Rossing T.D. 1992. *The Physics of Musical instruments.* Springer Verlag, New York.

[5] Välimäki,V., Karjalainen, M., and Laakso, T.I. 1993. Modeling of Woodwind bores with Finger Holes. *Proc. of the ICMC (1993)*, pp. 32–39.

[6] Van Duyne, S.A., Pierce, J.R., and Smith, J.O. 1994. Traveling Wave Implementation of A Losseles Mode-Coupling Filter and The Wave Digital Hammer. *Proc. of the ICMC (1994)*, pp. 411–418.

[7] Scavone, G.P. and Smith, J.O. 1997. Digital Waveguide Modeling of Woodwind toneholes. *Proc. of the ICMC (1997)*, pp. 260–263.

[8] Smith, J.O., and Scavone, G.P. 1997. The One-Filter Keefe Clarinet Tonehole. *Proc. of the IEEE workshop on Applications of Signal Processing to Audio and Acoustics (1997).* IEEE Press, New York.

[9] Scavone, G.P., and Cook, P.R. 1998. Real-time Computer Modeling of Woodwind Instruments. Proc. of the ISMA (1998), pp. 197–202.

[10] Barjau, A., Keefe, D.H., Cardona, S. 1999. Time-domain simulation of acoustical waveguides with arbitrarily spaced discontinuities. JASA, Vol. 105(3) (1999). pp. 1951–1962.

[11] Scavone, G.P. 1999. Modeling Wind Instrument Sound Radiation using Digital Waveguides. *Proc. of the ICMC (1999)*, pp. 355–358.